

The *Swift* capture of a long X-ray burst from XTE J1701–407

Manuel Linares,^{1*} Anna L. Watts,¹ Rudy Wijnands,¹ Paolo Soleri,¹
Nathalie Degenaar,¹ Peter A. Curran,¹ Rhaana L. C. Starling²
and Michiel van der Klis¹

¹*Astronomical Institute ‘Anton Pannekoek’, University of Amsterdam and Center for High-Energy Astrophysics, Kruislaan 403, NL-1098 SJ Amsterdam, Netherlands*

²*Department of Physics and Astronomy, University of Leicester, University Road, Leicester LE1 7RH*

Accepted 2008 October 8. Received 2008 September 30; in original form 2008 August 28

ABSTRACT

XTE J1701–407 is a new transient X-ray source discovered on 2008 June 8. More than one month later, it showed a rare type of thermonuclear explosion: a long type I X-ray burst. We report herein the results of our study of the spectral and flux evolution during this burst, as well as the analysis of the outburst in which it took place. We find an upper limit on the distance to the source of 6.1 kpc by considering the maximum luminosity reached by the burst. We measure a total fluence of 3.5×10^{-6} erg cm⁻² throughout the ~ 20 min burst duration and a fluence of 2.6×10^{-3} erg cm⁻² during the first two months of the outburst. We show that the flux decay is best fitted by a power law (index ~ 1.6) along the tail of the burst. Finally, we discuss the implications of the long burst properties, and the presence of a second and shorter burst detected by *Swift* ten days later, for the composition of the accreted material and the heating of the burning layer.

Key words: binaries: close – stars: neutron – X-rays: binaries – X-rays: bursts.

1 INTRODUCTION

The bulge of our Galaxy harbours a large fraction of the known population of accreting compact objects. During one of the regular monitoring observations of that region with the proportional counter array (PCA) onboard the *Rossi X-ray timing explorer* (*RXTE*) on 2008 June 8, a new transient X-ray source was discovered: XTE J1701–407 (Markwardt, Pereira & Swank 2008a). Three days later a follow-up observation with the X-ray telescope (XRT) onboard *Swift* improved the source localization and showed a spectrum that could be fitted with an absorbed power law of index ~ 2 (Degenaar & Wijnands 2008). The transient nature, flux level and spectrum of the source are characteristic of X-ray binaries, but the exact class of the binary (high mass or low mass) was unknown and the compact object [black hole or neutron star (NS)] remained unidentified for more than one month. On July 17 at 13:29:59 UT, the burst alert telescope (BAT) onboard *Swift* detected an X-ray flare at a position consistent with that of XTE J1701–407 (Barthelmy et al. 2008). *Swift* began slewing to the source 60 s after the trigger and the XRT began observing the field 97 s after the initial BAT trigger, detecting a fading X-ray source at the position of XTE J1701–407 (Barthelmy et al. 2008). Markwardt, Cummings & Krimm (2008b) suggested that the flare could be caused by a thermonuclear burst

based on the early BAT data. By studying the evolution of the XRT spectrum, Linares et al. (2008) found a clear cooling curve and confirmed the speculation that this was a thermonuclear event, identifying the source as an accreting NS and the system, in all likelihood, as a low-mass X-ray binary (LMXB). As noted by Linares et al. (2008) this particular event, having a total duration of more than 15 min, belongs to the rare subclass of long duration bursts (Cumming et al. 2006).

After the long X-ray burst, the source continued in outburst¹ and *RXTE* kept observing it. A refined *Swift*–XRT position (Starling & Evans 2008), a search for an infrared (IR) counterpart (Kaplan & Chakrabarty 2008) and the discovery of kHz quasi-periodic oscillations (QPOs; Strohmayer, Markwardt & Swank 2008) were all reported during the following two weeks. On July 27, BAT detected another X-ray flare from XTE J1701–407 (Sakamoto et al. 2008). The soft spectrum and duration (~ 10 s) of the flare indicated that this was a type I X-ray burst (http://gcn.gsfc.nasa.gov/notices_s/318166/BA/), and hereafter we refer to it as the short burst (even though from the BAT data, the total duration is somewhat uncertain). At the moment of writing

¹To clarify the terminology, we stress that in the context of LMXBs an outburst is powered by accretion and lasts for weeks to years whereas a type I X-ray burst, or ‘burst’, results from unstable thermonuclear burning on the surface of a NS and lasts for ~ 10 s to \sim hours.

*E-mail: linares@uva.nl

the source is still active, more than two months after the start of the outburst.

In this Letter, we present our analysis of the bursting behaviour of this source. Long bursts are rare, and therefore probe quite unusual burning regimes. Their duration is between that of normal Type I X-ray bursts (durations ~ 10 – 100 s, triggered by unstable burning of H/He) and superbursts (durations \sim hours, triggered by unstable burning of C). There are two scenarios in which such bursts could occur, both requiring the build-up and ignition of a thick layer of He. One possibility is that the system is ultracompact, so that it accretes nearly pure He (Cumming et al. 2006). The other possibility is that unstable H burning at low accretion rates builds up He (Peng, Brown & Truran 2007; Cooper & Narayan 2007). While several examples of the first type are now known (see e.g. in ’t Zand, Jonker & Markwardt 2007; Falanga et al. 2008, and references therein), the second class – which probe the boundaries of H burning stability – have so far proved much rarer (Chenevez et al. 2007). In this Letter, we will demonstrate that XTE J1701–407 is a good candidate for membership of this second class.

2 OBSERVATIONS AND DATA ANALYSIS

We analysed all the 27 pointed *RXTE*–PCA observations of XTE J1701–407 taken until 2008 August 10 (ID 93444-01). We also analysed the *Swift*–XRT data taken during and after the long burst (on July 17, observation ids 00317205000 and 00317205001). *Swift* observed XTE J1701–407 again on July 27, triggered by the BAT detection of the short burst (Section 1). We also included this XRT observation (observation id 00318166000) in our analysis, which started ~ 109 s after the trigger but did not detect the burst. In the following two sections, we provide the details of our analysis. All errors given in Section 3 correspond to the 1σ confidence level.

2.1 Swift

We ran the XRT pipeline (v. 0.12.0) on all the *Swift* observations. For the spectral analysis, we created exposure maps and ancillary files and used the latest response matrices (v011) provided by the *Swift*–XRT team. We grouped the spectra to a minimum of 20 counts per bin, applied a systematic error of 2.5 per cent (Campana et al. 2008) and fitted the 0.5–10 keV spectra within *XSPEC* (Arnaud 1996, v. 11). In our fits (see models below), we fixed the absorbing column density to the average value found from X-ray fits to the persistent emission: $3.5 \times 10^{22} \text{ cm}^{-2}$ (Degenaar & Wijnands 2008; Markwardt et al. 2008a).

Observation 00317205000 started on 2008 July 17 at 13:31:36.9 UT (Section 1) and lasted for a total of about 1 ks. All the XRT data were collected in windowed timing (WT) mode, except for the initial ~ 8 s which were taken in photon counting (PC) mode. We divided the observation into nine contiguous intervals of increasing length in order to compensate for the flux decay and maintain an approximately constant total number of counts in each interval (between ~ 1500 and ~ 2500). About 830 s after the start of the observation, a data gap of ~ 3300 s occurred, after which the XRT continued to observe the source for another ~ 35 s. This last data segment allows us to estimate the persistent flux after the X-ray burst. We extracted source and background spectra for each interval using circular regions with radii of ~ 30 and ~ 15 pixel, respectively, and fitted the resulting spectra using an absorbed blackbody model (reduced χ^2 between 0.7 and 1.1).

We performed fast Fourier transforms on 2 s segments of XRT–WT data taken during the long burst in order to search for rapid variability. For that purpose we used the energy range 0.5–10 keV, keeping the original time resolution and thereby sampling the ~ 0.5 –280 Hz frequency range.

Both post-burst observations (00317205001 and 00318166000) allow us to characterize the persistent soft X-ray emission of XTE J1701–407. For the PC data, we used an annular extraction region with radii 10–25 pixel in order to account for pileup. The energy fraction enclosed by the resulting annuli was about 20 per cent, and such energy loss was taken into account when creating the ancillary files. Finally, including also the WT data, we fitted the energy spectra with an absorbed power-law model (reduced χ^2 of 1.1 and 1.2).

2.2 RXTE

We analysed all the pointed *RXTE* observations of the source made until August 10. After applying standard filters we extracted energy spectra from Standard 2 data collected by PCU2 (Proportional Counter Unit 2) and corrected them for background using the latest PCA background models. We generated response matrices and fitted the spectra within *XSPEC* in the 3.0–25.0 keV band, after applying a 1 per cent systematic error, with a blackbody plus power-law model corrected for absorption (see Section 2.1). The resulting fits had reduced χ^2 between 0.5 and 1.4 (for 45 degrees of freedom). We extracted a hardness ratio (‘hard colour’ hereafter) for each observation, defined as the count rate in the 9.7–16.0 keV band divided by that in the 6.0–9.7 keV band and normalized by that of the Crab. Furthermore, we extracted a background and deadtime corrected HEXTE (High Energy X-ray Timing Experiment; cluster B) energy spectrum from each observation, but found no significant source emission above 50 keV in any of them.

3 RESULTS

3.1 Outburst

The overall light curve is shown in Fig. 1, together with the evolution of the hard colour. The outburst shows two peaks at a similar flux, $(6.2, 6.8) \times 10^{-10} \text{ erg cm}^{-2} \text{ s}^{-1}$. The BAT transient monitor light

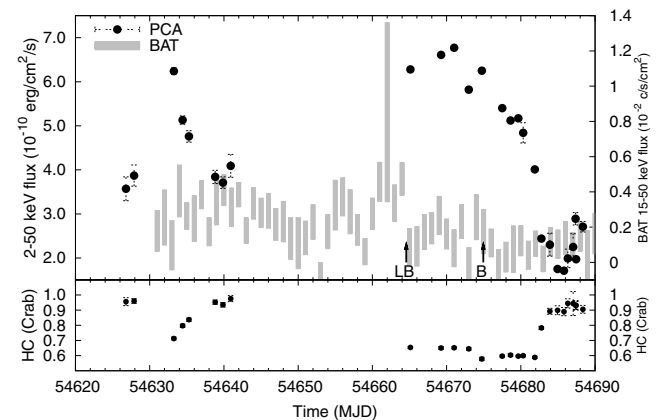


Figure 1. Time evolution of the 2–50 keV unabsorbed flux (top panel, filled dots) and the hard colour (bottom panel) during the outburst of XTE J1701–407, as measured by the *RXTE*–PCA. Arrows indicate the times of the long (LB) and short (B) X-ray burst. The 15–50 keV flux measured by *Swift*–BAT is shown as well (top panel, grey rectangles).

Table 1. Properties of both type I X-ray bursts detected from XTE J1701–407. Question marks indicate ill-constrained values.

	Long	Short
BAT rise time (s)	50	5
Duration ^a (min)	21	?
Peak flux ^b (10^{-8} erg s ⁻¹ cm ⁻²)	8.4	~4.9
Total fluence ^c (10^{-6} erg cm ⁻²)	3.5	?
Persistent flux ^d (10^{-10} erg s ⁻¹ cm ⁻²)	8.6 ± 0.9	9.8 ± 1.0

^aFrom start of rise to 1 per cent of peak flux.

^bBolometric.

^cIncluding fluence in BAT (Markwardt et al. 2008b) and during XRT data gap.

^dUnabsorbed 1–50 keV.

curves² indicate that the source was active during the three weeks where no *RXTE* pointed observations were obtained, at a flux level similar to that measured during the first two weeks of outburst (see Fig. 1). The hard colour traces directly the changes in spectral state along the outburst, with a clear tendency: when the source is bright its spectrum is soft whereas the spectrum is harder at the lowest fluxes. However, it is interesting to note that as is the case for many other NS–LMXBs the correspondence between flux and hardness is not one-to-one (van der Klis 2006). Together with the presence of kHz quasi-periodic oscillations (Strohmayer et al. 2008), the peak luminosity and the spectral evolution (Fig. 1) show that XTE J1701–407 is a new member of the atoll source class (Hasinger & van der Klis 1989). Both X-ray bursts occur at relatively high fluxes (see Table 1) and soft spectra (low hard colour).

By interpolating linearly between the available data points, we integrate the light curve and find a total outburst fluence up until August 10 of 2.6×10^{-3} erg cm⁻². More than half of this energy (1.6×10^{-3} erg cm⁻²) was radiated before the long burst occurred, whereas the fluence between long and short bursts was about 5×10^{-4} erg cm⁻².

From our spectral fits to the post-burst XRT observations (Section 2.1) we measure 2–10 keV fluxes of $(4.0 \pm 0.9) \times 10^{-10}$ erg cm⁻² s⁻¹ (July 17) and $(5.6 \pm 1.0) \times 10^{-10}$ erg cm⁻² s⁻¹ (July 27), which are consistent with the fluxes in the same band obtained from the nearest (within one day) PCA observations. In both the cases, the photon index was ~2. Furthermore, we estimate unabsorbed 1–2 keV fluxes of 2.3×10^{-10} erg cm⁻² s⁻¹ (July 17) and 3.5×10^{-10} erg cm⁻² s⁻¹ (July 27) and add them to the unabsorbed 2–50 keV fluxes measured with the PCA within one day of the bursts (6.3×10^{-10} erg cm⁻² s⁻¹ for both bursts; see Fig. 1). These 1–50 keV fluxes (Table 1) are the closest we can safely get to the bolometric persistent flux at the times of the bursts, but we note that the uncertainties in the absorbing column density and the extrapolation to the 0.01–1 keV energy range could change the bolometric flux by a factor of ~2 (see e.g. discussion in in’t Zand et al. 2007).

3.2 X-ray bursts

From the flux and spectral parameters reported by Markwardt et al. (2008b), we estimate a bolometric unabsorbed peak flux of 8.4×10^{-8} erg cm⁻² s⁻¹ for the long burst. By assuming that the peak luminosity was equal to or lower than that typical of photospheric expansion type I X-ray bursts ($\sim 3.8 \times 10^{38}$ erg s⁻¹; Kuulkers et al.

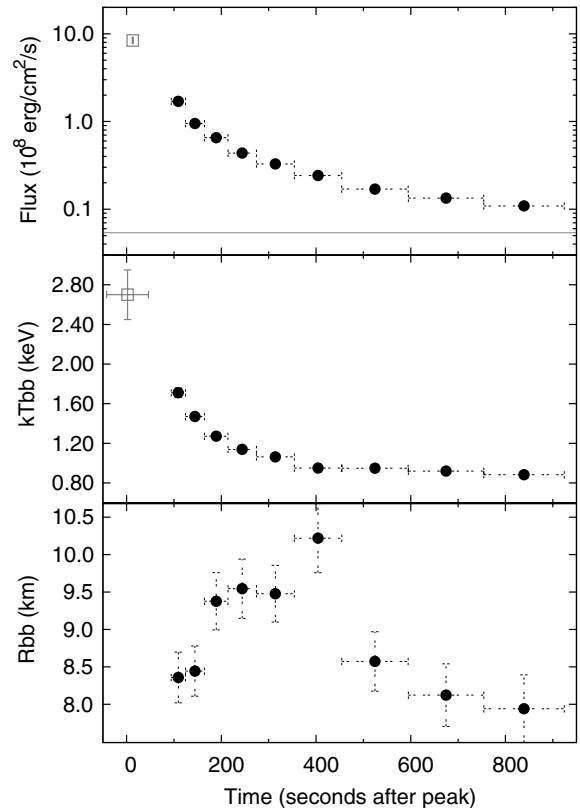


Figure 2. Time evolution of the bolometric flux (top panel), blackbody temperature (middle panel) and blackbody radius (bottom panel) along the long X-ray burst. Filled dots correspond to our *Swift*–XRT measurements whereas empty squares show *Swift*–BAT results (Markwardt et al. 2008b). The horizontal dotted line on the top panel indicates the persistent flux. Error bars in the x-axis represent the averaged intervals. The distance upper limit of 6.1 kpc has been used to obtain the blackbody radius.

2003) we can place an upper limit on the distance to the source of 6.1 kpc. On the other hand, if we use the Eddington limit for a mix of H and He ($\sim 1.6 \times 10^{38}$ erg s⁻¹ for a hydrogen fraction $X = 0.7$) as a limit for the peak luminosity, the upper limit on the distance becomes 4.0 kpc. The rise time in the BAT light curve was about 50 s, the peak occurred about 10 s after the trigger (http://gcn.gsfc.nasa.gov/notices_s/317205/BA/) and the total duration, assuming that the burst finished when it reached 1 per cent of the peak flux, was about 21 min. The fluxes in the post-burst XRT observation, taken more than 2 h after the peak of the long burst, are similar to the flux we measure in the last interval (~1 h after the peak, Section 2.1), confirming that the source had returned to the persistent level.

Fig. 2 shows the results of our time-resolved spectroscopy of the tail of the long burst. The flux decays by almost two orders of magnitude and the temperature decreases from 1.72 ± 0.05 to 0.88 ± 0.02 keV during the burst tail (see also Linares et al. 2008). XRT did not observe the peak of the burst, and no spectral variations were seen in BAT data of that period (Markwardt et al. 2008b). Therefore, the question of whether or not the burst showed photospheric radius expansion cannot be addressed. Going back to our XRT measurements, the radius of the blackbody appears to increase between ~200 and ~500 s after the peak (Fig. 2). However, the large error affecting this parameter, the uncertainties on the underlying model (NS atmosphere in a dramatically non-steady state) and the absence of an associated drop in the blackbody temperature imply

² <http://swift.gsfc.nasa.gov/docs/swift/results/transients/>

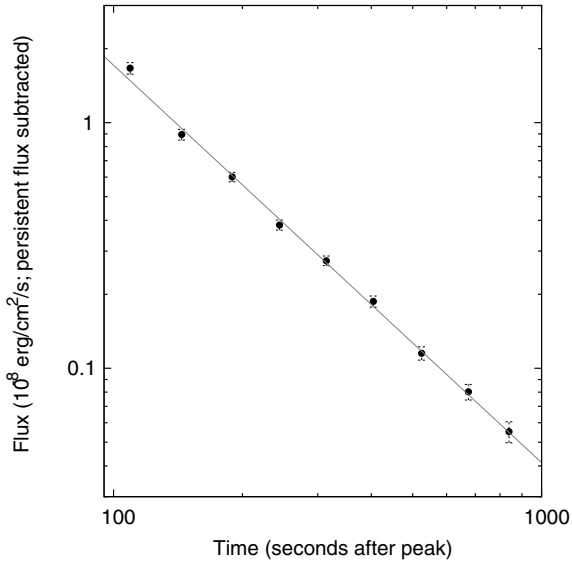


Figure 3. Fit to the long burst flux decay with a power law of index ~ 1.6 , together with the values of the baseline-subtracted bolometric flux.

that this cannot be taken as concrete evidence of a physical increase in emitting area.

We fit the flux decay of the long burst measured by the XRT and find that a simple power law with an index of -1.62 ± 0.04 and normalization $(3.0 \pm 0.6) \times 10^{-5} \text{ erg cm}^{-2} \text{ s}^{-1}$ gives a remarkably good description of the data (reduced χ^2 of 1.2; see Fig. 3). A simple or double exponential decay do not fit the data satisfactorily (reduced χ^2 of 22 and 7, respectively). We note that power-law cooling is consistent with the expectations from models for long bursts (Cumming & Macbeth 2004).

The bolometric fluence measured by XRT during the long burst, after subtracting the persistent flux level, is $2.2 \times 10^{-6} \text{ erg cm}^{-2}$. We integrate the flux decay along the data gap (Section 2.1) and estimate a fluence of $4.4 \times 10^{-7} \text{ erg cm}^{-2}$ during that period. Adding the reported BAT fluence (Markwardt et al. 2008b), we find a total burst fluence of $3.5 \times 10^{-6} \text{ erg cm}^{-2}$, which using the 6.1 kpc upper limit on the distance corresponds to a maximum radiated energy of $1.6 \times 10^{40} \text{ erg}$.

We searched the XRT power spectra obtained during the tail of the long burst (Section 2.1) and found no strong pulsations or QPOs. This non-detection is not surprising given (i) the distribution of burst oscillation frequencies (Galloway et al. 2008) combined with our Nyquist frequency ($\sim 280 \text{ Hz}$) and (ii) the relatively low count rate collected by the XRT: for the maximum rate of $\sim 90 \text{ count s}^{-1}$, a 3σ detection of a 2-Hz wide QPO in a 2 s FFT (fast Fourier transform) would require a fractional rms of at least ~ 25 per cent (van der Klis 1995), much higher than the values usually measured (Galloway et al. 2008).

4 DISCUSSION

Theoretical modelling of long bursts suggests that they involve the build-up and ignition of a thick layer of He. One possibility is that the binary is ultracompact, so that the accreted fuel is almost pure He. At low accretion rates, and in the absence of heating from steady H burning, the temperature remains low and ignition can be delayed until a thick layer of He has built up (in't Zand et al. 2005; Cumming et al. 2006). Although He burning is quick, the cooling

time is long because of the thickness of the layer in which the heat is deposited. Long bursts can also be triggered in systems accreting a mix of H and He if the source accretes at low rates, close to the point where H burning stabilizes (Fujimoto, Hanawa & Miyaji 1981; Peng et al. 2007; Cooper & Narayan 2007). In this case weak H flashes can build up He, which ignites sporadically, resulting in a long burst. Layer thickness again results in a long cooling time: but the presence of H in the burning mix may also prolong nuclear energy generation.

Using the measured fluxes F from Table 1 and the upper limit on the distance d that we obtained from the long burst, we infer an upper limit on the global accretion rate $\dot{M} \approx 4\pi d^2 R F / GM$ of $3.7 \times 10^{-10} M_{\odot} \text{ yr}^{-1}$ (for a NS mass $M = 1.4 M_{\odot}$ and radius $R = 10 \text{ km}$) around the times of the two bursts. Assuming isotropy, this corresponds to an upper limit on the local accretion rate \dot{m} of $1.9 \times 10^3 \text{ g cm}^{-2} \text{ s}^{-1}$ (2.5 per cent of the Eddington rate for an Eddington luminosity of $1.6 \times 10^{38} \text{ erg s}^{-1}$). This accretion rate is close to the rate where H burning is expected to transition to stability (Fujimoto et al. 1981; Peng et al. 2007; Cooper & Narayan 2007), so we need to examine both scenarios for the generation of the long burst.

The BAT rise time of the long burst, $\approx 50 \text{ s}$, is much longer than most of the pure He bursts examined by in't Zand et al. (2007) and Falanga et al. (2008). This points to it being a mixed H/He type burst, triggered by H ignition, although we note that burst light curves can change considerably depending on the energy range where they are observed (see Chelovekov, Grebenev & Sunyaev 2006; Molkov et al. 2005).

We next consider the ignition conditions. The long burst had a total energy output of at most $E_b = 1.6 \times 10^{40} \text{ erg}$ (6.1 kpc distance). The corresponding ignition column depth $y = E_b(1+z)/4\pi R^2 Q_{\text{nuc}}$, where z is the redshift, R the NS radius and $Q_{\text{nuc}} = 1.6 + 4X \text{ MeV nucleon}^{-1}$ the nuclear energy release, given an H fraction X at ignition (Galloway et al. 2008). Assuming $z = 0.31$ (the redshift for a $1.4 M_{\odot}$, 10 km radius NS), we derive an ignition depth $y = 3.9 \times 10^8 \text{ g cm}^{-2}$ for solar abundances ($X = 0.7$) and $y = 1.1 \times 10^9 \text{ g cm}^{-2}$ for pure He ($X = 0$). Ignition of pure He at this column depth would require a heat flux from the deep crust of $\gtrsim 2 \text{ MeV nucleon}^{-1}$ at 1 per cent Eddington accretion rates (fig. 22, Cumming et al. 2006). This is higher than the crustal energy release of $\sim 1.5 \text{ MeV nucleon}^{-1}$ calculated by Haensel & Zdunik (1990, 2003), but close to the value of $\sim 1.9 \text{ MeV nucleon}^{-1}$ recently found by Gupta et al. (2007) and Haensel & Zdunik (2008). Recent results by Horowitz, Dussan & Berry (2008) demonstrate that even larger amounts of heat may be released in the crust of an accreting NS. However, the high heat requirements certainly put some strong constraints on the pure He accretion scenario. Using the maximum local accretion rate calculated above ($1.9 \times 10^3 \text{ g cm}^{-2} \text{ s}^{-1}$), these ignition conditions predict minimum recurrence times $\Delta t_{\text{rec}} = y(1+z)/\dot{m}$ of $\sim 10 \text{ d}$ ($X = 0$) and $\sim 3 \text{ d}$ ($X = 0.7$). The data provide only weak constraints on the time without bursts that elapsed before the long burst (we estimate that the source was in the field of view of BAT for about 20 per cent of the two months analysed herein), but these numbers are at least compatible with the time since the start of the outburst.

The presence of a short, weaker burst at similar accretion rates is perhaps the strongest piece of evidence pointing to mixed H/He fuel. The short burst has a relatively slow rise time, $\approx 5 \text{ s}$, similar to that expected for mixed H/He bursts. The fact that it has a lower peak flux than the long burst also implies some H content: if the system were a pure He accretor we would expect both bursts to reach similar peak fluxes since He bursts, whether long or short, are expected to exhibit photospheric radius expansion (Cumming

2004). In the H-triggered burst scenario it is possible to have bursts with quite different properties at very similar accretion rates, as H burning transitions to stability (Cooper & Narayan 2007).

XTE J1701–407 increases the number of known NS-LMXBs in the interesting low accretion rate bursting regime. The balance of evidence suggests that it may be a good probe of thermonuclear burning near the boundary of stable H ignition. However, further observations, in particular better constraints on recurrence times and burst energetics, are required to confirm this picture. Identification of the companion star and determination of the orbital parameters may also be able to confirm whether or not the system is ultracompact.

ACKNOWLEDGMENTS

ML would like to thank C. Markwardt and A. Cumming for stimulating discussions and N. Rea, E. Martínez and Ll. Guasch for their encouraging comments. RLCS acknowledges support from STFC.

REFERENCES

- Arnaud K. A., 1996, in Jacoby G. H., Barnes J., eds, Proc. ASP Conf. Ser., Vol. 101, Astronomical Data Analysis Software and Systems V. Astron. Soc. Pac., San Francisco, p. 17
- Barthelmy S. et al., 2008, GCN, 7985, 1
- Campana S. et al., 2008, ApJ, 683, L9
- Chelovekov I. V., Grebenev S. A., Sunyaev R. A., 2006, Astron. Lett., 32, 456
- Chenevez J. et al., 2007, A&A, 469, L27
- Cooper R. L., Narayan R., 2007, ApJ, 661, 468
- Cumming A., 2004, Nucl. Phys. B. Proc. Supp., 132, 435
- Cumming A., Macbeth J., 2004, ApJ, 603, L37
- Cumming A., Macbeth J., in't Zand J. J. M., Page D., 2006, ApJ, 646, 429
- Degenaar N., Wijnands R., 2008, Astron. Telegram, 1572, 1
- Falanga M., Chenevez J., Cumming A., Kuulkers E., Trap G., Goldwurm A., 2008, A&A, 484, 43
- Fujimoto M. Y., Hanawa T., Miyaji S., 1981, ApJ, 247, 267
- Galloway D. K., Muno M. P., Hartman J. M., Psaltis D., Chakrabarty D., 2008, ApJS, in press (astro-ph/0608259)
- Gupta S., Brown E. F., Schatz H., Möller P., Kratz K.-L., 2007, ApJ, 662, 1188
- Haensel P., Zdunik J. L., 1990, A&A, 227, 431
- Haensel P., Zdunik J. L., 2003, A&A, 404, L33
- Haensel P., Zdunik J. L., 2008, A&A, 480, 459
- Hasinger G., van der Klis M., 1989, A&A, 225, 79
- Horowitz C. J., Dussan H., Berry D. K., 2008, Phys. Rev. C, 77, 045807
- in't Zand J. J. M., Cumming A., van der Sluys M. V., Verbunt F., Pols O. R., 2005, A&A, 441, 675
- in't Zand J. J. M., Jonker P. G., Markwardt C. B., 2007, A&A, 465, 953
- Kaplan D. L., Chakrabarty D., 2008, Astron. Telegram, 1630, 1
- Kuulkers E., den Hartog P. R., in't Zand J. J. M., Verbunt F. W. M., Harris W. E., Cocchi M., 2003, A&A, 399, 663
- Linares M., Soleri P., Curran P., Wijnands R., Degenaar N., van der Klis M., Starling R., Markwardt C., 2008, Astron. Telegram, 1618, 1
- Markwardt C. B., Pereira D., Swank J. H., 2008a, Astron. Telegram, 1569, 1
- Markwardt C. B., Cummings J., Krimm H., 2008b, Astron. Telegram, 1616, 1
- Molkov S., Revnivtsev M., Lutovinov A., Sunyaev R. A., 2005, A&A, 434, 1069
- Peng F., Brown E. F., Truran J. W., 2007, ApJ, 654, 1022
- Sakamoto T. et al., 2008, GCN, 8034, 1
- Starling R., Evans P., 2008, Astron. Telegram, 1621, 1
- Strohmayer T. E., Markwardt C. B., Swank J. H., 2008, Astron. Telegram, 1635, 1
- van der Klis M., 1995, A. Kiziloglu, J. van Paradijs, eds, Proc. NATO Advanced Study Institute on the Lives of Neutron Stars. Kluwer Academic, Dordrecht, p. 301
- van der Klis M., 2006, in Lewin W. H. G., van der Klis M., eds, Compact Stellar X-ray Sources. Cambridge Univ. Press, Cambridge, p. 39

This paper has been typeset from a \LaTeX file prepared by the author.